Hindawi Publishing Corporation
Mathematical Problems in Engineering
Volume 2015, Article ID 795092, 9 pages
http://dx.doi.org/10.1155/2015/795092

Research Article

Time Reversal Reconstruction Algorithm Based on PSO Optimized SVM Interpolation for Photoacoustic Imaging

Mingjian Sun, Zhenghua Wu, Ting Liu, Jiajun Hu, Guanqun Wu, and Naizhang Feng

Department of Control Science and Engineering, School of Astronautics, Harbin Institute of Technology, Room H618, Main Building, No. 2 West Wenhua Road, Weihai, Shandong 264209, China

Correspondence should be addressed to Mingjian Sun; sunmingjian@hit.edu.cn

Received 9 November 2014; Revised 25 March 2015; Accepted 22 April 2015

Academic Editor: Javier Plaza

Photoacoustic imaging is an innovative imaging technique to image biomedical tissues. The time reversal reconstruction algorithm in which a numerical model of the acoustic forward problem is run backwards in time is widely used. In the paper, a time reversal reconstruction algorithm based on particle swarm optimization (PSO) optimized support vector machine (SVM) interpolation method is proposed for photoacoustics imaging. Numerical results show that the reconstructed images of the proposed algorithm are more accurate than those of the nearest neighbor interpolation, linear interpolation, and cubic convolution interpolation based time reversal algorithm, which can provide higher imaging quality by using significantly fewer measurement positions or scanning times.

1. Introduction

Recently, photoacoustic tomography (PAT) has emerged as a powerful imaging technology for many biomedical applications [1, 2]. PAT is able to provide functional imaging of physiological parameters. Photoacoustic imaging combines electromagnetic and ultrasonic wave synergistically, providing relatively deep speckle-free imaging with high electromagnetic contrast at high ultrasonic resolution. In PAT, the developing reconstruction methods have been an important task [3, 4]. Various reconstruction methods, such as filtered backprojection, Fourier transform, alternative algorithm, time reversal, inversion of the linear Radon transform, and delay and sum beamforming, have been developed under different assumptions and approximation [5–9]. Besides, different shaped measurement surfaces will lead to different shaped final artifacts.

In a word, the image reconstruction progress can be regarded as running a numerical model of forward problem backwards in time domain, at each time step, in which the measured time-varying pressure signals are enforced (in time reversed order) as a Dirichlet boundary condition at their recorded positions that is called time reversal reconstruction method. It has been described as the "least restrictive" imaging algorithm on the basis that it relies on fewer assumptions than many other imaging reconstruction algorithms [10, 11]. The idea of time reversal to PAT was suggested by Fink and Prada [12] and later used for PAT by Xu and Wang [13], and the time reversal method was applied to deriving exact and approximate reconstruction algorithms for PAT in an arbitrary configuration and heterogeneous acoustic media.

In conventional time reversal imaging reconstruction, the recorded pressure time series are enforced in time reversed order as a Dirichlet boundary condition as the position of detectors on the measurement surface. If a sparse array of the detectors points is used to collect the measurement rather than a continuous surface, the enforced time reversed boundary condition will necessarily be discontinuous. This can cause significant blurring in the reconstructed images. To solve the problem, Treeby and Cox [14] improved time reversal image reconstruction by using interpolated sensor data. In the course, the interaction can be avoided by interpolating the recorded data onto a continuous rather than discrete measurement surface within the k-space grid used for the reconstruction. The edges of the reconstructed image are considerably sharper and the magnitude has also been improved. After that, Cox and Treeby [15] used the enforced

time reversal boundary condition to trap artifacts in the final image, and by truncating the data, or introducing an adaptive threshold boundary condition, this artifact trapping can be mitigated to some extent.

In this paper, what we are concerned with in the method is the artifacts elimination and interaction of image reconstruction when using "time reversal" algorithm. An optimized hybrid interpolation algorithm has been used to create a continuous surface that is spatially equivalent to the original Cartesian measurement surface via interpolation. It is demonstrated that the proposed algorithm can reduce artifact and improve the acoustic magnitude and the signal-to-noise ratio through partial correction for the discontinuous aperture.

2. Theory and Methods

2.1. Acoustic Propagation Theory in PAT. For PAT, in a lossless acoustic medium, the photoacoustic wave equation can be reformulated as an initial value problem. The photoacoustic forward problem may be written as

$$\left[\frac{\partial^2}{\partial t^2} - c(x)^2 \rho(x) \nabla \cdot \left(\frac{1}{\rho(x)} \nabla\right)\right] p(x,t) = 0, \quad (1)$$

where the initial conditions are given by

$$\begin{aligned} p(x,t)\big|_{t=0} &= p_0(x), \\ u(x,t)\big|_{t=0} &= \left.\frac{\partial p}{\partial t}\right|_{t=0} = 0, \end{aligned} \quad (2)$$

where $p(x,t)$ is the acoustic pressure at time $t \in R^+$ and point $x \in \Omega \subset R^n$ inside the imaging region Ω, $u(x,t)$ is the acoustic particle velocity, $c_0(x)$ is the sound speed, and $\rho(x,t)$, $\rho_0(x)$ are the acoustic and ambient densities, respectively. Using this framework, it is straightforward to modify the adiabatic equation of state to account for acoustic absorption or nonlinear effects.

2.2. Time Reversal Image Reconstruction. In PAT, the photoacoustic image reconstruction problem is to estimate the initial pressure distribution $p_0(x)$ inside the imaging region Ω given measurement of $p(x,t)$ on arbitrary measurement surface S. In time reversal imaging, this estimate is achieved by using the recorded measurements $p_m(x_S,t)$ of the acoustic pressure $p(x_S,t)$ over an arbitrary surface $x_S \in S$ for some time $t = 0$ to T. In this case, the initial pressure in (2) is set to zero, giving

$$\begin{aligned} p(x,t)\big|_{t=0} &= 0, \\ u(x,t)\big|_{t=0} &= 0 \\ p(x_S,t) &= p_m(x_S, T-t). \end{aligned} \quad (3)$$

From the equation, the pressure in the imaging field Ω from $t = 0$ to T can be obtained; at the same time, the reverse-time variable t from $t = 0$ to T also can be computed. In a practical sense, the reconstruction is performed by using the acoustic pressure time histories measured on S for $t = 0$ to T in time reversed order as an enforced (time-varying) Dirichlet boundary condition on $\widehat{S}$ within a numerical acoustic propagation model. Here, $\widehat{S} \subset \widehat{\Omega}$ and both $\widehat{S}$ and $\widehat{\Omega}$ are in silico equivalents to the real world S and Ω.

During the time reversal reconstruction, if ρ and c vary spatially, the time reversed waves will no longer interfere precisely to reproduce the original wave field, which will lead to the production of additional waves. The extra waves are called vestigial waves, which are the time reversed vestiges of the scattered waves. Vestigial waves are artifact-producing waves, in the sense that any of them remaining in the computational domain would constitute artifacts in the final PAT image. To improve the reconstruction result of the discontinuous aperture, the artifacts and interaction can be largely removed by interpolating the recorded data onto a continuous measurement surface within the k-space grid used for the reconstruction. As an optimized hybrid interpolation algorithm, PSO optimized SVM interpolation algorithm can provide higher convergence rate and optimization precision, which has been used to create a continuous surface that is spatially equivalent to the original Cartesian measurement surface via interpolation to solve the problem.

2.3. PSO Optimized SVM Interpolation Algorithm. The essence of the support vector machine (SVM) training parameter selection is a process of optimization search [16]. In the process of interpolation, the index of the training model of the support vector machine, such as the fitting precision and the generalization ability, is directly related to the selection of the nuclear function, nuclear parameter, the penalty coefficient, and other parameters in the parameter optimization algorithm [17].

The particle swarm optimization (PSO) algorithm is a kind of bionic optimization algorithm, which is derived from the approximation behavior simulation of birds and fish population. It is an optimization tool based on iteration, searching for the optimal solution through the collaboration of the individual particles. The algorithm has a strong ability in global optimization. Using the particle swarm optimization algorithm to solve the optimization problem is equal to the search for the space location of a bird. The birds in the space are called "particles." Each particle adjusts its flight path randomly based on the flight experience of its own so as to close to the optimal point finally. Different particle has different location and speed and individual fitness corresponding to the flight objective function. The flight path is adjusted by tracking two "extreme values." One of the extreme values is called individual extremum which indicates the optimal solution of the particle itself. The other one is the global extremum, which indicates the optimal solution of the whole swarm. When the two extreme values are found, the particles update their speed and locations as follows:

$$\begin{aligned} v_{id}(t+1) &= w v_{id}(t) + c_1 \mathrm{rand}_1(i)\left(p_{id}(t) - x_{id}(t)\right) \\ &\quad + c_2 \mathrm{rand}_2(i)\left(p_{gd}(t) - x_{id}(t)\right) \\ x_{id}(t+1) &= x_{id}(t) + v_{id}(t+1), \end{aligned} \quad (4)$$

where w is the inertia weight; t is the current evolutionary iteration time; $i = 1, 2, \ldots, m$, $d = 1, 2, \ldots, n$; $\text{rand}_1(i)$ and $\text{rand}_2(i)$ are random numbers distributed in the interval $[0, 1]$; m is the swarm size; c_1 and c_2 are the accelerating factors; $x_{id}(t)$ is the d-dimension component of the location of the ith particle in the t iteration; $v_{id}(t)$ is the d-dimension component of the velocity of the ith particle in the t iteration; $p_i = (p_{i1}, p_{i2}, \ldots, p_{in})$ is the individual extreme value; $p_{id}(t)$ is the d-dimension component of the best location of the ith particle; $p_g = (p_{g1}, p_{g2}, \ldots, p_{gn})$ is the global extreme value; $p_{gd}(t)$ is the d-dimension component of the best location of the swarm.

Using the particle swarm optimization algorithm to solve the optimization problem is mainly discussing the optimization problem of the penalty factor c, insensitive parameter γ, and the nuclear parameter σ. The progress of PSO-SVM method is shown in Figure 1. In general, the parameters of C, γ, and σ are related with learning samples and practical problems. The penalty factor C controls the degree of punishment when samples are misclassified and achieves a compromise between training error and model complexity. The larger C is, the higher fitting precision is required. It makes training so difficult and also takes a longer time. But when C is smaller, it will lower the fitting precision. Too big or too small value of C will deteriorate the generalization capability of the system; the former is called "overlearning," and the latter is called "less learning." The insensitive parameter γ reflects the regression model's sensitivity of the noise included in input variable. The larger γ is, the lower model fitting accuracy and complexity is also prone to overfit. The nuclear parameter σ represents the mean square error of Gaussian function and is the width of function in independent variables direction. When σ is smaller, the kernel function has better fitting performance, but it will deteriorate the generalization ability. So, using the particle swarm optimization algorithm to solve the optimization problem is mainly discussing the optimization problem of the penalty factor c, insensitive parameter γ, and the nuclear parameter σ.

In the process of the SVM interpolation, the solution data in solution space cannot be solved by PSO algorithm directly. The right way is to encode it and convert to particle string structure of the searching space to solve the optimization problem. In the process of the optimization, there are three optimization parameters to be solved, which mean that the dimension of the particle location is three, as (c, γ, σ). Then the real value encoding is used, m 3d particles x_{id} represent the initiate location of the particles swarm, and it is randomly generated according to the optimal interval of parameters. The random number v_{id} generated in $[0, 1]$ is the initial speed. There exists an updating problem of different range in the parameter optimization of speed and locations of the particles swarm. At this time, we should do the normalized mapping process for the three parameters before the optimization process. And after the updating, the inverse normalized process will be done to the original scope. In the iterating process, fixed evolution algebra is set. In the solving process, the maximum value will be compared with the fixed value in each generation; the operation will be terminated when the two values reach an agreement.

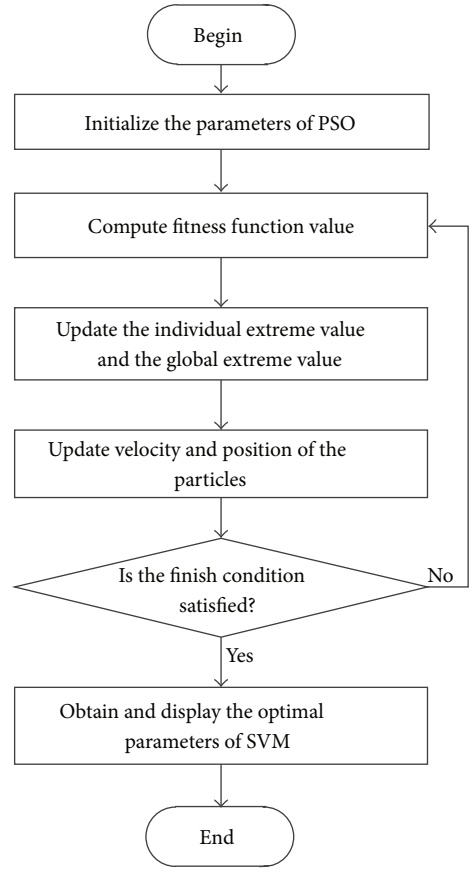

Figure 1: The process of specification of PSO-SVM method.

3. Results and Discussion

3.1. Time Reversal Reconstruction Algorithm. The initial pressure distribution of a phantom (simulating tumor tissue) with a 256×256 pixel grid is shown in Figure 2(a). The conventional time reversal algorithm is used to reconstruct the PAT phantom, and the result is shown in Figure 2(b). It shows that the reconstructed PAT image has been significantly blurred due to the discontinuous boundary condition, and some artifacts have been caused by vestigial waves. Figure 3 shows a profile of the initial pressure and the conventional reconstruction pressure, which facilitates a large amplitude gap between them.

3.2. Time Reversal Reconstruction Based on PSO-SVM Interpolation Method. The algorithm above is slow for real-time applications. Recently fast PSO optimized SVM interpolation algorithm has been developed [18, 19]. These algorithms can be employed for real-time algorithm implementation. In time reversal PAT imaging, an interpolation function is often employed to compute missed Cartesian raster pixel values. The well-known interpolation algorithms are linear interpolation, cubic convolution interpolation, and cubic spline

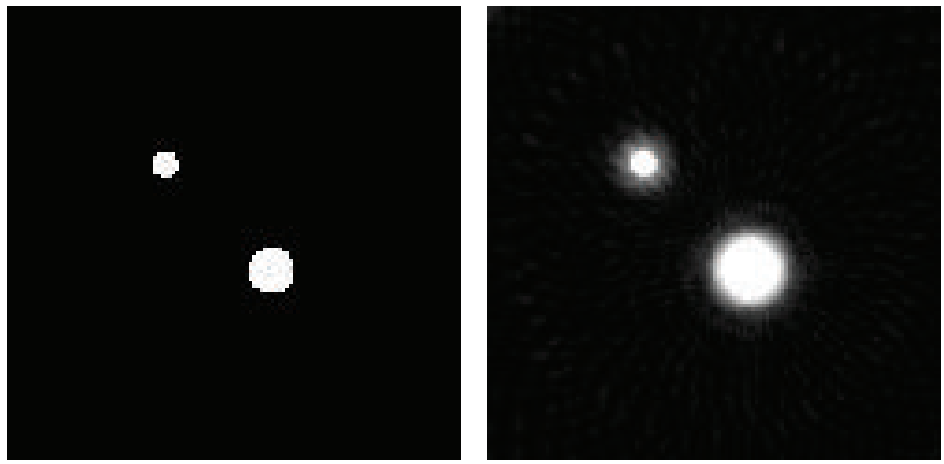

(a) (b)

Figure 2: PAT image of phantom: (a) initial pressure distribution; (b) conventional time reversal reconstruction.

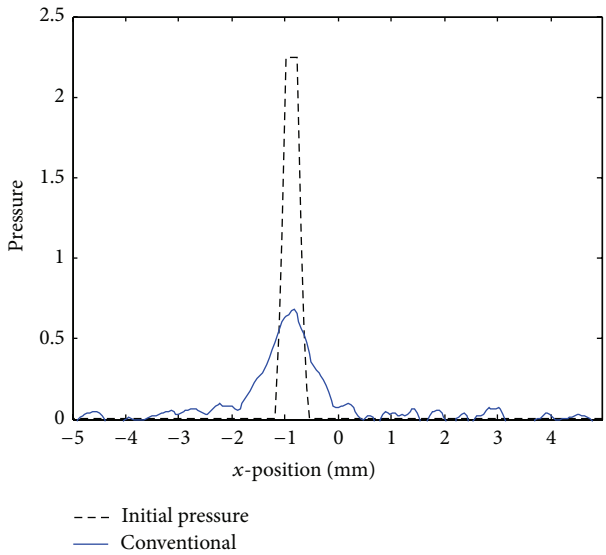

Figure 3: Pressure distribution of initial pressure and conventional time reversal reconstruction.

interpolation algorithm, which can be applied to reconstruct the PAT images. To prove the effectiveness and superiority of the proposed method in PAT image reconstruction, a two-dimensional photoacoustic image simulation experiment is given to illustrate the effect of the imaging performance by using various interpolation based time reversal algorithms. Therefore, the initial pressure distribution, the sound heterogeneity, and the measure surface will choose simple geometrical shape; the generation process of the photoacoustic signal will be simulated by K-Wave Matlab toolbox.

The simulation is performed on grid architecture with 5% and 15% Gaussian White Noise (GWN) added to the recorded photoacoustic data, respectively. The PC with Intel P6300 CPU and 4 GB RAM is used in the simulation. The propagation velocity of sound in the medium is 1500 m/s, the medium density is 1000 kg/m^3, and the initial pressure distribution is the two locations in the spherical absorber at (x, z). For a central position at (150, 150), the diameter is 1.3 mm and for the other central position at (90, 90), the diameter is 0.8 mm. A single array ultrasonic detector is put around the absorber selection for a round from the grid (0, 0). The collected photoacoustic signal which was measured at multiple points is used for reconstruction; the result images of different interpolations applied to time reversal algorithm using 30 measurement points are displayed in Figures 4(a)–4(f). In Figure 4, Figure 4(a) represents ideal image of light sound absorber, Figure 4(b) represents reconstruction image of conventional time reversal reconstruction algorithm, and Figures 4(c)–4(f) are reconstruction images of using time reversal reconstruction algorithm based on linear interpolation, three cubic interpolations, cubic spline interpolation, and PSO optimized SVM interpolation algorithm. When less measurement points are used, the collected photoacoustic data imperfection between each measurement point is not enough, and pseudowave is generated in the reconstruction process. It demonstrates that PSO optimized SVM interpolation is able to preserve more edges information in detailed regions and remove more artifacts (blurring) than the other approaches.

The results of 50 measurement points are shown in Figure 5. It demonstrates that the more measurement points are, the better reconstruction image quality we get. It can be seen from the photoacoustic reconstruction images that the PSO optimized SVM interpolation algorithm can preserve more original image details and remove the artifact phenomenon better; thus it will be most effective to apply it to the time inversion algorithm. This is also evident in Figure 6, which shows a profile through the center of the two absorbers. The junction between the absorber (simulated tumor) and the background is noticeably sharper after the interpolation compared to before, especially for the PSO optimized SVM interpolation we utilized. The overall magnitude of the proposed reconstruction has also been improved

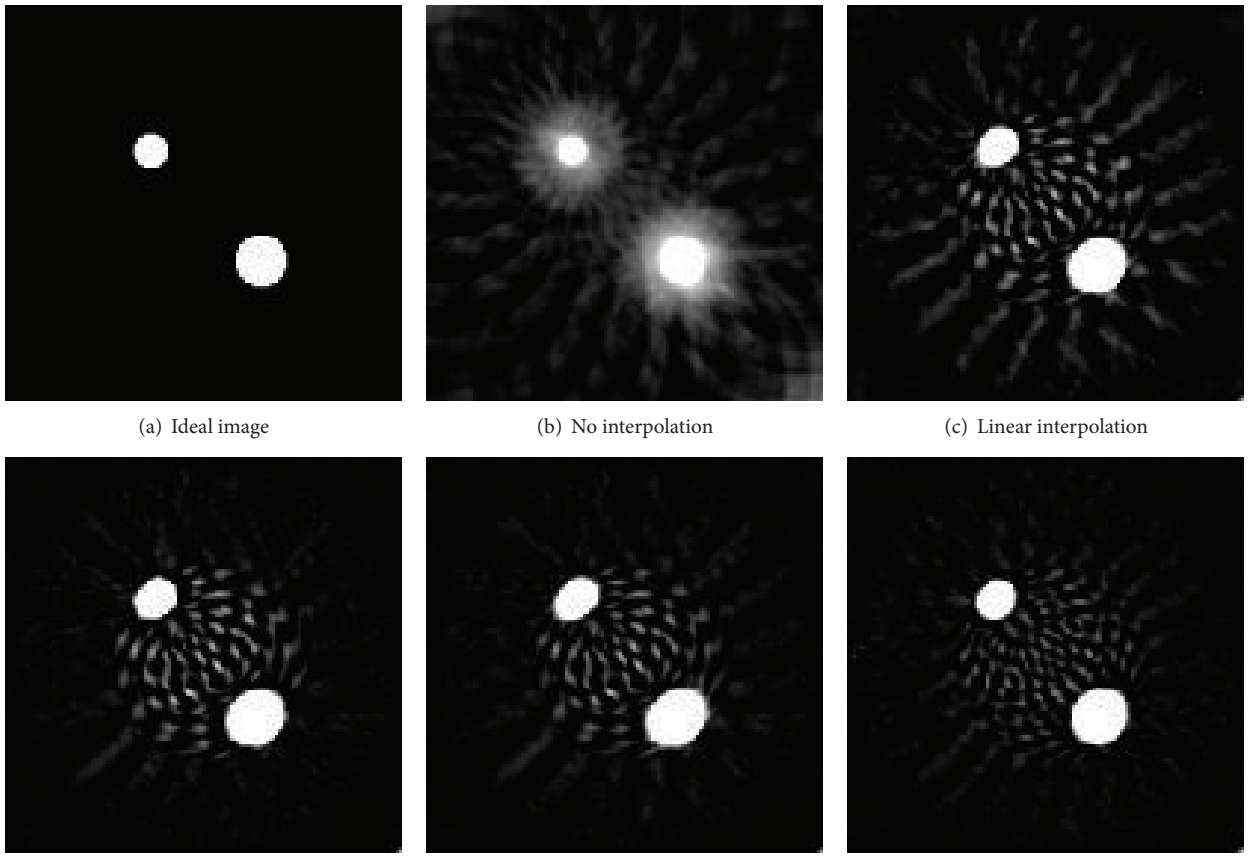

(a) Ideal image (b) No interpolation (c) Linear interpolation

(d) Three cubic interpolations (e) Cubic spline interpolation (f) PSO optimized SVM interpolation

Figure 4: Reconstruction result based on different interpolation methods (30 measurements, 5% noise).

Table 1: Reconstruction performance of different interpolation methods on time reversal algorithm (5% noise).

Time reversal method	MSE (30)	PSNR (30)	TIME (30)/s	MSE (50)	PSNR (50)	TIME (50)/s
Conventional	0.3221	1.7114	0	0.1904	3.9955	0
Linear interpolation	0.1362	5.4504	0.1097	0.0498	9.8149	0.1091
Cubic convolution interpolation	0.1317	5.5954	0.0099	0.0490	9.8876	0.0100
Cubic spline interpolation	0.1220	5.9287	0.0122	0.0480	9.9752	0.0124
PSO optimized SVM interpolation	0.0765	7.9569	0.4958	0.0240	12.9815	0.4977

through partial correction for the attention effect. The quality of the reconstruction images (with 30, 50 measurements added with 5%, 15% GWN, resp.) is measured via mean square error (MSE) and peak signal-to-noise ratio (PSNR), which are shown in Tables 1 and 2. It also demonstrates that the PSO optimized SVM interpolation is the most accurate interpolation for time reversal method to reconstruct PAT images. The experiment shows that the proposed method can significantly improve the image resolution and suppress the artifacts when less measurement points are used in a single-element photoacoustic detector imaging system.

A tissue phantom is built and shown in Figure 7(a). The phantom is irradiated by a laser and observed; the photoacoustic images were reconstructed by filter backprojection (FBP) algorithm, conventional time reversal algorithm, and PSO optimized SVM time reversal algorithm using 50 and 100 measurements. Results depicted in Figures 7(b)–7(g) indicate that the reconstruction of the photoacoustic image from PSO optimized SVM time reversal algorithm represents the best performance, which can obtain more source-image details than conventional time reversal algorithm and has less artifacts than FBP algorithm, and this makes it a suitable algorithm for PAT.

In our experiment, the observed sample is 3D polyacrylamide gel (8% acrylamide + 0.5% bisacrylamide) with graphite powder in a standard culture dish (PN: 16235-1SGP, 35 × 12 (mm); diameter: 20 mm). The sample for the optical scanning includes 4 graphite spots (different graphite granule distributions) in different layers. The transducer is one single-element unfocused transducer with 40 MHz center frequency. The image of the sample is shown in Figure 8(a). Figures 8(b)–8(e) show the photoacoustic result

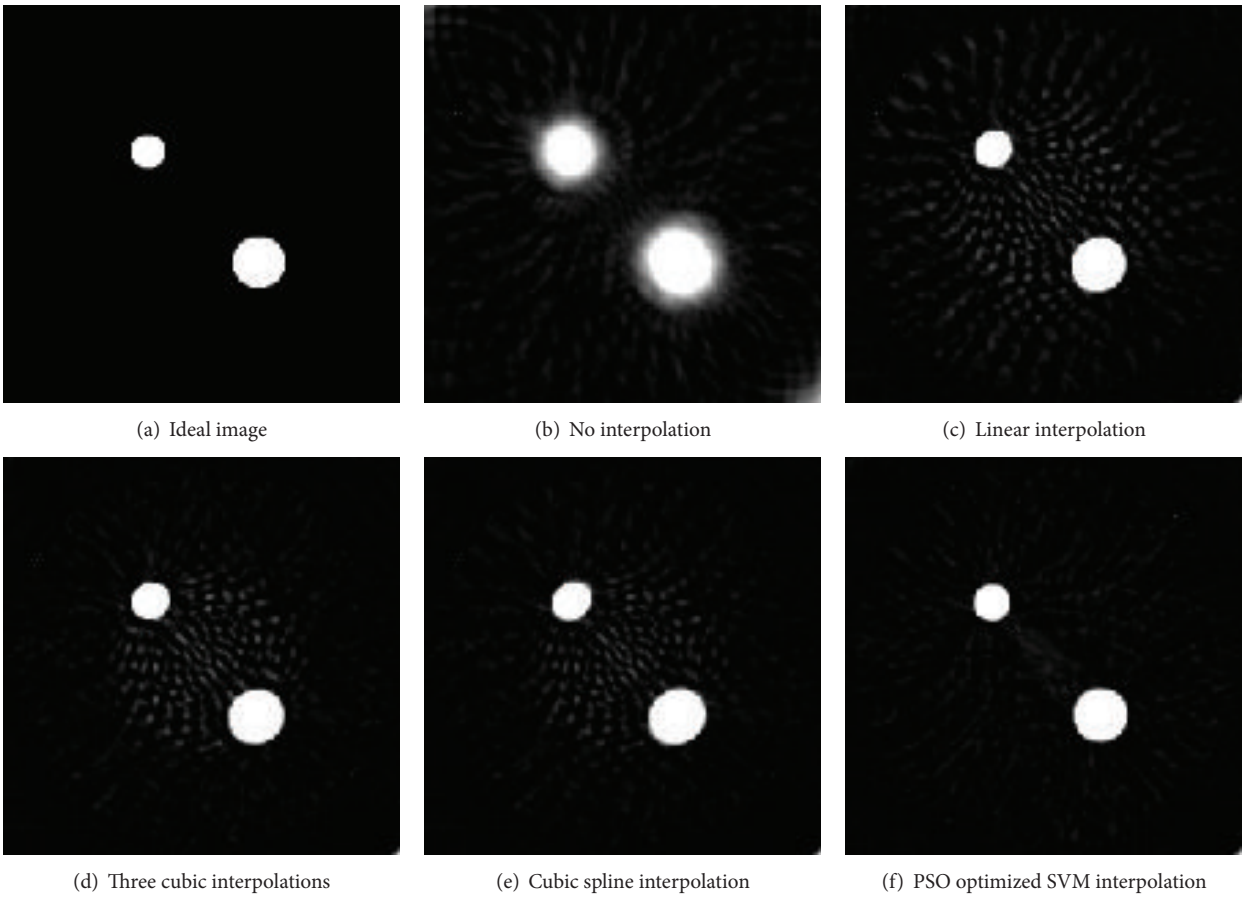

(a) Ideal image (b) No interpolation (c) Linear interpolation

(d) Three cubic interpolations (e) Cubic spline interpolation (f) PSO optimized SVM interpolation

Figure 5: Reconstruction result based on different interpolation methods (50 measurements, 5% noise).

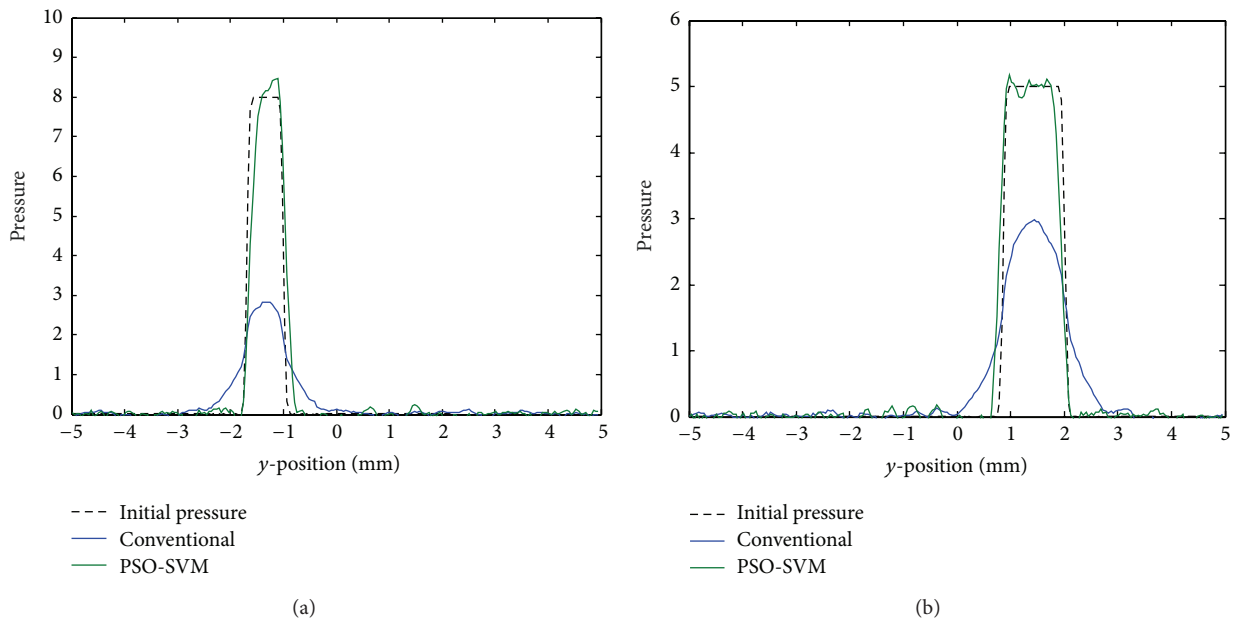

Figure 6: Comparisons of pressure distribution: (a) small spherical absorber; (b) big spherical absorber.

Table 2: Reconstruction performance of different interpolation methods on time reversal algorithm (15% noise).

Time reversal method	MSE (30)	PSNR (30)	TIME (30)/s	MSE (50)	PSNR (50)	TIME (50)/s
Conventional	0.3230	1.7000	0	0.1913	3.9749	0
Linear interpolation	0.1384	5.3813	0.1094	0.0522	9.6185	0.1090
Cubic convolution interpolation	0.1336	5.5324	0.0101	0.0511	9.7049	0.0105
Cubic spline interpolation	0.1236	5.8695	0.0121	0.0498	9.8194	0.0123
PSO optimized SVM interpolation	0.0776	7.8775	0.4978	0.0255	12.7833	0.4979

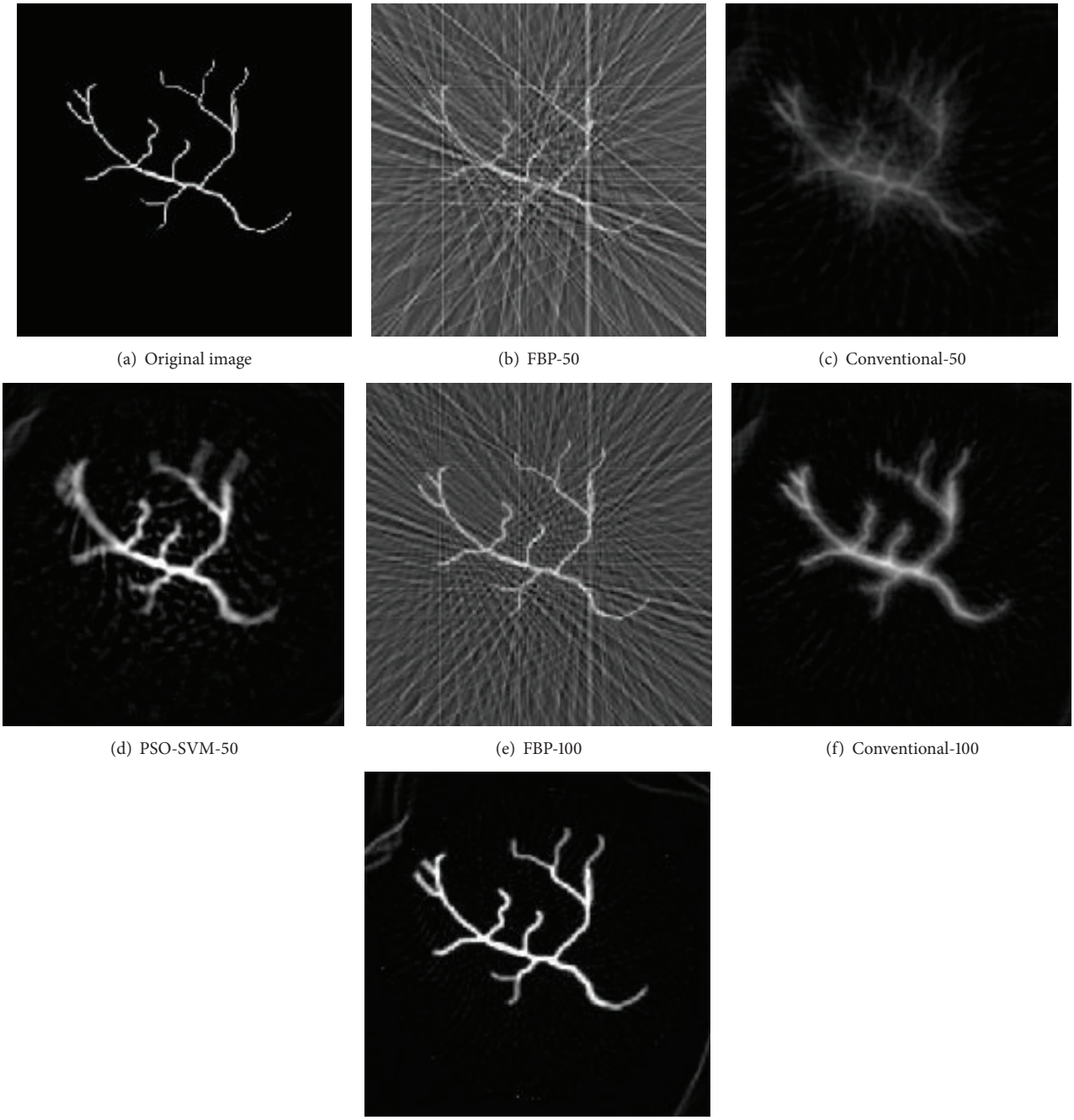

(a) Original image (b) FBP-50 (c) Conventional-50

(d) PSO-SVM-50 (e) FBP-100 (f) Conventional-100

(g) PSO-SVM-100

Figure 7: Reconstruction result based on different methods (50 and 100 measurements, 15% noise).

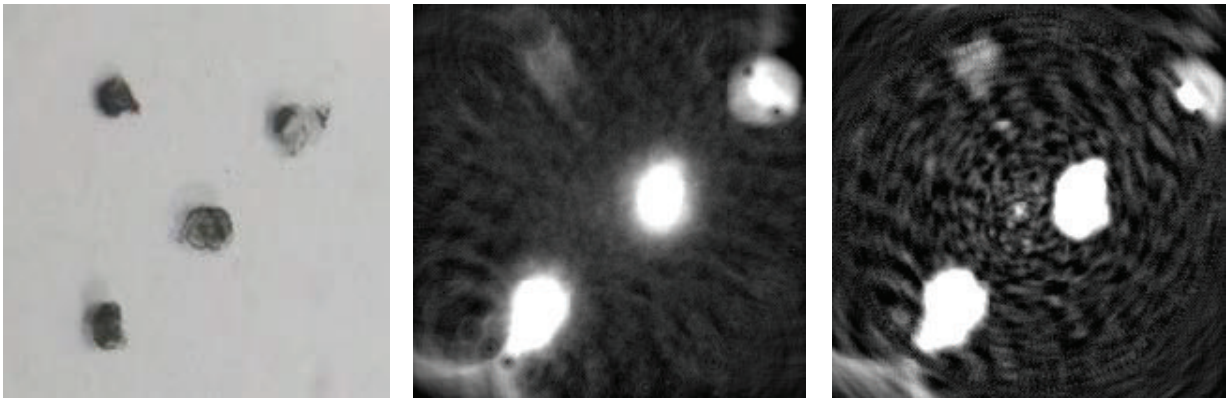

(a) Image of samples (b) Conventional-50 (c) PSO-SVM-50

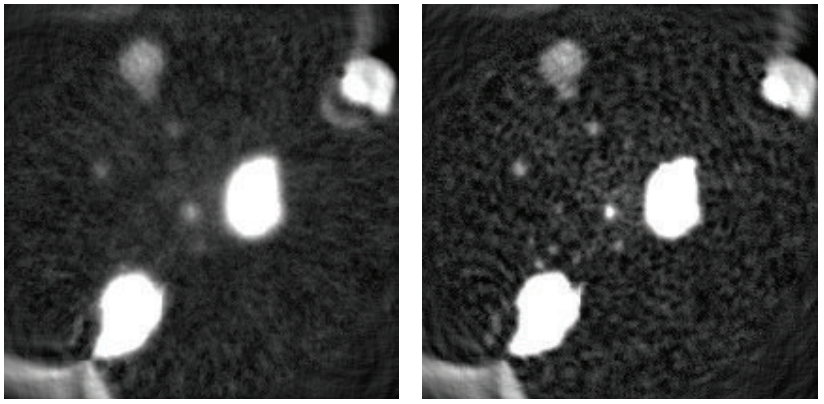

(d) Conventional-100 (e) PSO-SVM-100

Figure 8: Reconstruction result of PA experiment (50 and 100 measurements).

reconstructed by conventional time reversal algorithm and PSO optimized SVM time reversal algorithm using 50 and 100 measurements. As expected, the PSO optimized SVM reconstruction result holds the best performance of enhancing spatial resolution for more accurate image details of the absorption of graphite powder distribution.

4. Discussion

In practical photoacoustic imaging, the measurement surface is often incomplete or irregular. When a discrete measured surface is used, the time reversal algorithm fixes the acoustic pressure at these incomplete points which can make them act as optic point scatters, which may scatter back into the imaging region. This can result in arc-like artifacts across the image. One way to reduce the artifacts is to interpolate the measured data to a complete measurement surface acting as the boundary in time reverse course. The PSO optimized SVM interpolation method is used in the time reversal reconstruction algorithm. Compared with other interpolation methods, the method has higher convergence rate and optimization precision. In the course of interpolation, the optimized method can effectively eliminate the phenomenon of contour jaggies and blurring. With better parameter selection, training course, and more measurements, the method can keep more original image details and remove the artifact phenomenon better. In a word, after time reversal reconstruction, both the image magnitude and resolution are improved, so the proposed method can accurately compensate for the effects of acoustic absorption in incomplete photoacoustic imaging.

5. Conclusions

The primary contribution of this paper is a time reversal algorithm based on PSO optimized SVM interpolation which is proposed to produce more accurate reconstructed PAT images. The proposed method will reduce background interpolation artifacts and blurring in the PAT image at the expense of computational speed. What is more, the algorithm is capable of correcting the attention effect. The effectiveness of the algorithm is verified with the simulation. Also the PSO optimized SVM interpolation based time reversal algorithm can be used for medical PAT imaging system to obtain high resolution.

Conflict of Interests

The authors declared that there is no conflict of interests regarding the publication of this paper.

Acknowledgments

This research is supported by the National Natural Science Foundation of China (Grants no. 61201307 and no. 61371045) and the Fundamental Research Funds for the Central Universities (Grant no. HIT. NSRIF. 2013132).

References

[1] M. H. Xu and L. V. Wang, "Photoacoustic imaging in biomedicine," *Review of Scientific Instruments*, vol. 77, no. 4, Article ID 041011, 22 pages, 2006.

[2] L. V. Wang, "Prospects of photoacoustic tomography," *Medical Physics*, vol. 35, no. 12, pp. 5758–5767, 2008.

[3] Y. Xu, L. V. Wang, G. Ambartsoumian, and P. Kuchment, "Reconstructions in limited-view thermoacoustic tomography," *Medical Physics*, vol. 31, no. 4, pp. 724–733, 2004.

[4] P. Kuchment and L. Kunyansky, "Mathematics of thermoacoustic tomography," *European Journal of Applied Mathematics*, vol. 19, no. 2, pp. 191–224, 2008.

[5] M. H. Xu and L. V. Wang, "Universal back-projection algorithm for photoacoustic computed tomography," *Physical Review E*, vol. 71, no. 1, Article ID 016706, 7 pages, 2005.

[6] B. T. Cox, S. R. Arridge, and P. C. Beard, "Photoacoustic tomography with a limited-aperture planar sensor and a reverberant cavity," *Inverse Problems*, vol. 23, no. 6, pp. S95–S112, 2007.

[7] R. A. Kruger, P. Liu, Y. R. Fang, and C. R. Appledorn, "Photoacoustic ultrasound (PAUS)—reconstruction tomography," *Medical Physics*, vol. 22, no. 10, pp. 1605–1609, 1995.

[8] Y.-X. Su, R. K. K. Wang, F. Zhang, and J.-Q. Yao, "Two-dimensional photoacoustic imaging of blood vessel networks within biological tissues," *Chinese Physics Letters*, vol. 23, no. 2, pp. 512–515, 2006.

[9] C. G. A. Hoelen and F. F. M. De Mul, "Image reconstruction for photoacoustic scanning of tissue structures," *Applied Optics*, vol. 39, no. 31, pp. 5872–5883, 2000.

[10] Y. Hristova, P. Kuchment, and L. Nguyen, "Reconstruction and time reversal in thermoacoustic tomography in acoustically homogeneous and inhomogeneous media," *Inverse Problems*, vol. 24, no. 5, Article ID 055006, 2008.

[11] Y. Hristova, "Time reversal in thermoacoustic tomography—an error estimate," *Inverse Problems*, vol. 25, no. 5, Article ID 055008, 2009.

[12] M. Fink and C. Prada, "Acoustic time-reversal mirrors," *Inverse Problems*, vol. 17, no. 1, pp. R1–R38, 2001.

[13] Y. Xu and L. V. Wang, "Time reversal and its application to tomography with diffracting sources," *Physical Review Letters*, Article ID 033902, 2004.

[14] B. E. Treeby and B. T. Cox, "k-Wave: MATLAB toolbox for the simulation and reconstruction of photoacoustic wave fields," *Journal of Biomedical Optics*, vol. 15, no. 2, Article ID 021314, 2010.

[15] B. T. Cox and B. E. Treeby, "Artifact trapping during time reversal photoacoustic imaging for acoustically heterogeneous media," *IEEE Transactions on Medical Imaging*, vol. 29, no. 2, pp. 387–396, 2010.

[16] M. Liyong, S. Yi, and M. Jiachen, "Local spatial properties based image interpolation scheme using SVMs," *Journal of Systems Engineering and Electronics*, vol. 19, no. 3, pp. 618–623, 2008.

[17] T.-C. Ho and B. Zeng, "Super-resolution images by support vector regression on edge pixels," in *Proceedings of the International Symposium on Intelligent Signal Processing and Communications Systems (ISPACS '07)*, pp. 674–677, IEEE, Xiamen, China, December 2007.

[18] C. Li, Y. Liu, A. Zhou, L. Kang, and H. Wang, "A fast particle swarm optimization algorithm with cauchy mutation and natural selection strategy," in *Advances in Computation and Intelligence*, vol. 4683 of *Lecture Notes in Computer Science*, pp. 334–343, 2007.

[19] M.-Y. Shieh, J.-S. Chiou, Y.-C. Hu, and K.-Y. Wang, "Applications of PCA and SVM-PSO based real-time face recognition system," *Mathematical Problems in Engineering*, vol. 2014, Article ID 530251, 12 pages, 2014.